Active Control Experiment Study of a Flexible Beam with Multiple Time Delays

Chen Long-Xiang and Cai Guo-Ping

Department of Engineering Mechanics, Shanghai Jiaotong University, Shanghai 200240, P.R. China

(Received 25 April 2013; accepted 3 March 2014)

In this paper, active control for vibration of a flexible beam with multiple time delays is studied numerically and experimentally. Piezoelectric (PZT) patches are used as actuators, and foil gauges were used as sensors. Firstly the motion equation of a flexible beam with multiple time delays and Piezoelectric patches is presented and written into a state space form. Then the state equation is discretized and transformed into a standard form without any explicit time delay by a particular augmentation for state variables. So time-delay controller could be designed based on the standard state equation using the discrete active control method. Finally, numerical and experimental studies are presented to verify the validity of the time-delay processing method using the discrete optimal control method and the discrete variable structure control method, respectively. An experimental setup is constructed using DSP TMS320F2812. The numerical and experimental results show that the proposed time-delay controller is effective in suppressing the beam vibration. It is also applicable to both short- and long- time delays.

1. INTRODUCTION

Time delay exists inevitably in active control systems. It may make the actuator input energy into the controlled systems when energy is not needed. This may cause the degradation of control efficiency or even the instability of control systems.[1] Therefore, the research on time delay is of important theoretical significance and practical value.

Generally, the investigations on time delay may be divided into two classes: elimination and utilization technologies. At first, time delay was regarded as a "bad" factor that had only negative side effect on control systems. In order to eliminate or weaken the effect of time delay, some methods were subsequently proposed, including Taylor series expansion, phase shift technique and state pre-estimation.[2–4] These methods can deal effectively with some short time delay problems in control systems, but awkwardly with long ones. Cai and Huang have proposed a new time-delay controller.[5,6] This controller is designed directly from time-delay differential equation without any hypothesis in whole process of controller design, applicable for both short and long time delays. Chen proposed a theoretical method for a flexible beam with multiple time delays using the discrete optimal control.[7] Sun has recently proposed a continuous time approximation method for linear and nonlinear dynamical systems with time delay.[8] The key point of the methods mentioned above to eliminate the negative effect of time delay is so-called time-delay elimination technology or time-delay compensation technology. Its main function is to eliminate or weaken the negative effect of time delay on control efficiency. On the other hands, recent investigations have shown that voluntary introduction of delay into control systems can also benefit the control. For example, in nonlinear dynamics area, achievement is remarkable using time delay to control chaos motion.[9] Daqaq, Alhazza and Arafat studied the effect of feedback delays on the non-linear vibration of a cantilever beam.[10] In structural control area, Hosek and Olgac developed a time-delay resonator that may be used for vibration control of structures.[11] Cavdaroglu and Olgac considered the cart-and-pendulum system as research object, this study shows that systems with multiple delays may exhibit better performance by increasing the delays to more desirable levels.[12] Liu, Haraguchi, and Hu presents a reduction-based linear quadratic control for the dynamic system with a constant or a slowly time-varying input delay.[13] In robotics area, Cai and Lim designed a time-delay controller for a flexible manipulator and their results show that delayed feedback control design may possibly achieve much better control efficiency than the no-delay control design.[14] In control system of pipeline transport, time delay may be utilized to enhance steady critical speed of flowing liquid.[15] Time delay may be also used to improve system stability.[16,17] Those researches above involving the active utilization of time delay is so-called time-delay utilization technology, which assumes time delay as a design parameter to obtain good control performance. Although up to now researches have been done much on the elimination and utilization of time delay, most of work is theoretical one but few on experiment.

In this paper, Piezoelectric (PZT) patches are used as actuators, foil gauges as sensors, active control for vibration of a flexible beam with multiple time delays is studied numerically and experimentally. The controller with time delays is designed using the discrete optimal control method and the discrete variable structure control method, respectively. The feasibility and efficiency of the time-delay controller are verified theoretically and experimentally. This paper is organized

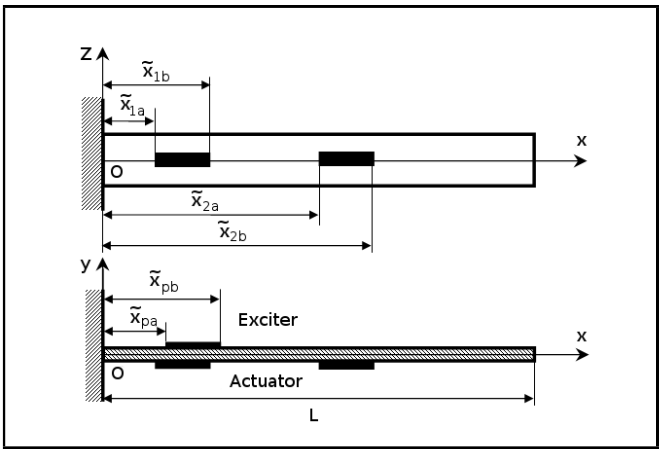

Figure 1. Cantilever beam model and the locations of PZT patches.

as follows. Section 2 presents the motion equation of flexible cantilever beam with time delays. The design of time-delay controller is described in Section 3. Section 4 gives the experimental scheme. The numerical and experimental results are shown in Section 5 in the consideration of the time-delay controller in this paper. Finally, concluding remarks are given in Section 6.

2. MOTION EQUATION

The transverse vibration of a flexible cantilever beam is considered, as shown in Fig. 1. The beam has a constant cross-section area with every center inertia axis being in the same plane, xoy. One PZT patch is used as exciter to initiate beam-forced vibration, and two PZT patches were used for controlling the vibration. The control forces produced by the two PZT actuators have different delays λ_1 and λ_2. Based on the Euler-Bernoulli hypothesis and using modal orthogonality, the i-th modal equation may be deduced as

$$\begin{aligned} &\ddot{\varphi}_i(t) + 2\zeta_i\omega_i\dot{\varphi}_i(t) + \omega_i^2\varphi_i(t) = \\ &\sum_{j=1}^{2} K_z[Y'_i(\tilde{x}_{ja}) - Y'_i(\tilde{x}_{jb})]V_j(t-\lambda_j) \\ &+K_z[Y'_i(\tilde{x}_{pa}) - Y'_i(\tilde{x}_{pb})]V_p(t); \qquad (1) \end{aligned}$$

$i = 1, 2, \cdots, \infty$ where $\varphi_i(t)$ is the i-th modal coordinate; ω_i is the natural frequency of the i-th mode; ζ_i is the i-th modal damping ratio; $Y_i(x)$ is the normalized modal shape corresponding to the i-th mode; $\tilde{x}_{ja}$ and $\tilde{x}_{kb}$ are the locations of the j-th PZT actuator on the beam, j = 1, 2; V_j is the applied voltage on the j-th PZT actuator; $\tilde{x}_{pa}$ and $\tilde{x}_{pb}$ are the locations of the PZT exciter; V_p is the applied voltage on the PZT exciter; and K_z is the constant value related to the physics and geometry characteristics of PZT material, may be found in.[7,18]

3. DESIGN OF MULTIPLE TIME-DELAY CONTROLLER

The first two vibration modes are considered to be controlled using the two PZT actuators in this paper. So, the modal equation can be written as

$$\ddot{\mathbf{\Phi}}(t)+\mathbf{C}\dot{\mathbf{\Phi}}(t)+\mathbf{K}\mathbf{\Phi}(t) = \sum_{j=1}^{2}\mathbf{H}_j V_j(t-\lambda_j)+\mathbf{H}_p V_p(t); \quad (2)$$

where $\mathbf{\Phi}(t) = [\varphi_1(t), \varphi_2(t)]^{\mathrm{T}}$,
$\mathbf{C} = diag(2\zeta_1\omega_1, 2\zeta_2\omega_2)$,
$\mathbf{K} = diag(\omega_1^2, \omega_2^2)$,
$\mathbf{H}_j = K_z[Y_1'(\tilde{x}_{ja}) - Y_1'(\tilde{x}_{jb}), Y_2'(\tilde{x}_{ja}) - Y_2'(\tilde{x}_{jb})]^{\mathrm{T}}$, and
$\mathbf{H}_p = K_z[Y_1'(\tilde{x}_{pa}) - Y_1'(\tilde{x}_{pb}), Y_2'(\tilde{x}_{pa}) - Y_2'(\tilde{x}_{pb})]^{\mathrm{T}}$.

In the state-space representation, Eq. (2) becomes

$$\dot{\mathbf{Z}}(t) = \mathbf{A}\mathbf{Z}(t) + \sum_{j=1}^{2}\mathbf{B}_j V_j(t-\lambda_j) + \mathbf{B}_p V_p(t); \qquad (3)$$

where $\mathbf{Z}(t) = \begin{bmatrix} \mathbf{\Phi}(t) \\ \dot{\mathbf{\Phi}}(t) \end{bmatrix}, \mathbf{A} = \begin{bmatrix} 0 & I \\ -\mathbf{K} & -\mathbf{C} \end{bmatrix}$,
$\mathbf{B}_j = \begin{bmatrix} 0 \\ \mathbf{H}_j \end{bmatrix}, \mathbf{B}_p = \begin{bmatrix} 0 \\ \mathbf{H}_p \end{bmatrix}$.

3.1. Discretization and Standard of Multiple Time-Delay Control Equation

Equation (3) is a time-delay differential equation that is inconvenient for control design. Here we consider the discretization and standard of this equation. The time delay λ_j can be written as

$$\lambda_j = l_j\bar{T}; \qquad (4)$$

where $\bar{T}$ is data sampling period and $l_j > 1$ is a positive integral number.

Zero-order holder is used in the structure, i.e.

$$V_j(t) = V_j(k), k\bar{T} \leqslant t < (k+1)\bar{T}; \qquad (5)$$

where k represents the k-th step of control and $V_j(k)$ denotes $V_j(kT)$. Equation (5) represents that the actuators exert constant control forces on the beam during two adjoining sampling points. This is feasible because data sampling period is usually very small.

Using Eq. (5), Eq. (3) becomes[7,19]

$$\mathbf{Z}(k+1) = \mathbf{F}\,\mathbf{Z}(k) + \sum_{j=1}^{2}\mathbf{G}_j V_j(k-l_j) + \mathbf{G}_p V_p(k); \quad (6)$$

where $\mathbf{F} = e^{\mathbf{A}\bar{T}}$, $\mathbf{G}_j = \int_0^{\bar{T}} e^{\mathbf{A}\eta}\mathrm{d}\eta\mathbf{B}_j$, $\mathbf{G}_p = \int_0^{\bar{T}} e^{\mathbf{A}\eta}\mathrm{d}\eta\mathbf{B}_p$, and $\mathbf{G}_{11} = \int_0^{\bar{T}} e^{\mathbf{A}\eta}\mathrm{d}\eta$.

Augmenting the state variables in Eq. (6) as

$$\begin{cases} Z_{4+1}(k) = V_1(k-l_1) \\ \vdots \\ Z_{4+l_1}(k) = V_1(k-1) \\ Z_{4+l_1+1}(k) = V_2(k-l_2) \\ \vdots \\ Z_{4+l_1+l_2}(k) = V_2(k-1) \end{cases}; \tag{7}$$

and defining a new state vector as

$$\bar{\mathbf{Z}}(k) = [\ \mathbf{Z}(k),\quad Z_{4+1}(k),\quad \cdots,\quad Z_{4+l_1+l_2}(k)\ ]^{\mathrm{T}}; \tag{8}$$

Thus Eq. (6) can be changed into the following standard discrete form without any explicit time delay:

$$\bar{\mathbf{Z}}(k+1) = \bar{\mathbf{F}}\bar{\mathbf{Z}}(k) + \bar{\mathbf{G}}\mathbf{V}(k) + \bar{\mathbf{G}}_p V_p(k); \tag{9}$$

where $\mathbf{V}(k) = [V_1(k),\ V_2(k)]^{\mathrm{T}}$,

$$\bar{\mathbf{F}} = \begin{bmatrix} \mathbf{F} & \mathbf{G}_1 & 0 & \cdots & 0 & \mathbf{G}_2 & 0 & \cdots & 0 \\ 0 & 0 & 1 & \cdots & 0 & 0 & 0 & \cdots & 0 \\ \vdots & \vdots & \vdots & \ddots & \vdots & \vdots & \vdots & \cdots & \vdots \\ 0 & 0 & 0 & \cdots & 1 & 0 & 0 & \cdots & 0 \\ 0 & 0 & 0 & \cdots & 0 & 0 & 0 & \cdots & 0 \\ 0 & 0 & 0 & \cdots & 0 & 0 & 1 & \cdots & 0 \\ \vdots & \vdots & \vdots & \cdots & \vdots & \vdots & \vdots & \ddots & \vdots \\ 0 & 0 & 0 & \cdots & 0 & 0 & 0 & \cdots & 1 \\ 0 & 0 & 0 & \cdots & 0 & 0 & 0 & \cdots & 0 \end{bmatrix},$$

$$\bar{\mathbf{G}} = \begin{bmatrix} 0 & 0 \\ 0 & 0 \\ \vdots & \vdots \\ 0 & 0 \\ 1 & 0 \\ 0 & 0 \\ \vdots & \vdots \\ 0 & 0 \\ 0 & 1 \end{bmatrix}, \bar{\mathbf{G}}_p = \begin{bmatrix} \mathbf{G}_p \\ 0 \\ \vdots \\ 0 \\ 0 \\ 0 \\ \vdots \\ 0 \\ 0 \end{bmatrix}.$$

Equation (9) is a standard discrete state equation that contains no time delay. The sufficient condition for stability of Eq. (9) is that all the eigenvalues of $\bar{\mathbf{F}}$ is within a unit circle. The system (9) is controllable provided that the matrix $[\bar{\mathbf{F}}, \bar{\mathbf{G}}]$ is controllable. When the system is controllable, the controllers can be designed. Next, the optimal control method and the variable structure control method will be used to design the controllers. Compared to other controller method, these two controllers can be simply designed. In addition, the optimal control can guarantee optimal control efficiency of systems, and the variable structure control method has strong robustness, and is insensitive for system parameters and external disturbances, and this method has good stability.

3.2. Controller Design using Optimal Control Method

Here we consider the controller design using the classical optimal control strategy. In the optimal controller design, external excitation term is neglected. The following performance index is used:

$$J = \int_0^\infty [\mathbf{Z}^{\mathrm{T}}(t)\bar{\mathbf{Q}}_1\mathbf{Z}(t) + \mathbf{V}^{\mathrm{T}}(t)\bar{\mathbf{Q}}_2\mathbf{V}(t)]\,\mathrm{d}t; \tag{10}$$

where $\bar{\mathbf{Q}}_1$ is non-negative definite symmetric matrix and $\bar{\mathbf{Q}}_2$ is positive definite symmetric matrix. The performance index is a continuous form so as to guarantee good response efficiency of systems not only on every sampling point but also between any two adjacent sampling points. However, the discrete performance index can only guarantee good efficiency on every sampling point and surge behavior may possibly exist between sampling points. So the continuous performance index is used as the objective function in this paper. Now the task of control design is to design controller for the system Eq. (3) such that the performance index in Eq. (10) attains minimum. In the above, Eq. (3) has been discretized and changed into the standard discrete form without any explicit time delay. Below the performance index will be discretized and changed to be the function of the augmented state.

Equation (10) may be written as the following discrete form

$$J = \sum_{k=1}^{\infty} J_k, J_k = \int_{k\bar{T}}^{(k+1)\bar{T}} [\mathbf{Z}^{\mathrm{T}}(t)\bar{\mathbf{Q}}_1\mathbf{Z}(t) + \mathbf{V}^{\mathrm{T}}(t)\bar{\mathbf{Q}}_2\mathbf{V}(t)]\,\mathrm{d}t; \tag{11}$$

The performance index in (11) may be rearranged as the following form:[7,19]

$$J = \sum_{k=0}^{\infty} [\bar{\mathbf{Z}}^{\mathrm{T}}(k)\hat{\mathbf{Q}}_1\bar{\mathbf{Z}}(k) + \mathbf{V}^{\mathrm{T}}(k)\hat{\mathbf{Q}}_2\mathbf{V}(k)]; \tag{12}$$

where $\hat{\mathbf{Q}}_1$ and $\hat{\mathbf{Q}}_2$ are given by

$$\hat{\mathbf{Q}}_1 = \begin{bmatrix} \mathbf{Q}_1 & \mathbf{Q}_{01} & 0 & \mathbf{Q}_{02} & 0 \\ \mathbf{Q}_{01}^{\mathrm{T}} & Q_{11} & 0 & Q_{12} & 0 \\ 0 & 0 & 0 & 0 & 0 \\ \mathbf{Q}_{02}^{\mathrm{T}} & Q_{21} & 0 & Q_{22} & 0 \\ 0 & 0 & 0 & 0 & 0 \end{bmatrix}, \hat{\mathbf{Q}}_2 = \mathbf{Q}_2; \tag{13}$$

where

$$\begin{cases} \mathbf{Q}_1 = \displaystyle\int_0^{\bar{T}} \mathbf{F}^{\mathrm{T}}(t)\bar{\mathbf{Q}}_1\mathbf{F}(t)\,\mathrm{d}t, \quad \mathbf{Q}_2 = \bar{\mathbf{Q}}_2\bar{T} \\ \mathbf{Q}_{0i} = [\displaystyle\int_0^{\bar{T}} \mathbf{F}^{\mathrm{T}}(t)\bar{\mathbf{Q}}_1\mathbf{G}_{11}(t)\,\mathrm{d}t]\mathbf{B}_i, \quad i = 1,2 \\ Q_{ij} = \mathbf{B}_i^{\mathrm{T}}[\displaystyle\int_0^{\bar{T}} \mathbf{G}_{11}^{\mathrm{T}}(t)\bar{\mathbf{Q}}_1\mathbf{G}_{11}(t)\,\mathrm{d}t]\mathbf{B}_j, \quad i,j = 1,2 \end{cases}; \tag{14}$$

and where $\mathbf{F}(t) = e^{At}$ and $\mathbf{G}_{11}(t) = \int_0^t e^{A\tau}d\tau$.

Equation (12) is a standard discrete form of performance index. So the next work is to design an optimal controller for the system in (9) by minimizing the objective function given by Eq. (12). This controller may be designed using the discrete optimal control method, given by

$$\begin{aligned}\mathbf{V}(k) &= -\mathbf{L}\,\bar{\mathbf{Z}}(k)\\ &= -\mathbf{L}_1\mathbf{Z}(k) - \mathbf{L}_2 V_1(k-l_1) - \cdots - \mathbf{L}_{l_1+1}V_1(k-1);\\ &- \mathbf{L}_{l_1+2}V_2(k-l_2)\cdots - \mathbf{L}_{l_1+l_2+1}V_2(k-1)\end{aligned} \tag{15}$$

where $\mathbf{L}_1(i = 1, \cdots, l_1+l_2+1)$ are the component matrices of $\mathbf{L}$. We can observe from Eq. (15) that the controller contains not only the current step of state feedback term, but also the linear combination of some former steps of controls. Since the time-delay controller is designed directly from the time-delay differential equation and no approximation or hypothesis involved, it tends to guarantee the stability of control systems, and is suitable for both small time delay and large time delay.

3.3. Controller Design using Variable Structure Method

The variable structure control method is known as the sliding mode control method, where sliding mode is the remarkable characteristics of this control method. The controller can be obtained by using the discrete reaching condition. The phase trajectory of the system will move toward the switching surface in finite time, and then reaching the origin point or the equilibrium position until the system reaches stabilization.

In the variable structure control method, a linear switching function is considered

$$\mathbf{S}(\bar{\mathbf{Z}}) = \mathbf{C}\bar{\mathbf{Z}}; \tag{16}$$

where $\mathbf{C}$ is undetermined coefficient vector of the switching function. $\mathbf{S}(\mathbf{Z}) = \mathbf{C}\mathbf{Z} = \mathbf{0}$ is the linear switching surface.

The discrete approach law is given by[20]

$$\mathbf{S}(k+1) - \mathbf{S}(k) = -\varepsilon\bar{T}\,\mathrm{sgn}[\mathbf{S}(k)] - q\bar{T}\,\mathbf{S}(k); \tag{17}$$

where $\bar{T}$ is the sampling period, $\epsilon > 0$, $q > 0$ and $q\bar{T} < 1$.

From Eqs. (9) and (16), the left-hand term of Eq. (17) can be further written as

$$\mathbf{S}(k+1) - \mathbf{S}(k) = \mathbf{C}[\bar{\mathbf{F}}\,\bar{\mathbf{Z}}(k) + \bar{\mathbf{G}}\,\mathbf{V}(k) + \bar{\mathbf{G}}_p\mathbf{V}_p(k)] - \mathbf{C}\bar{\mathbf{Z}}(k); \tag{18}$$

Hence the controller can be obtained from Eqs. (17) and (18) and written as

$$\begin{aligned}\mathbf{V}(k) = [\mathbf{C}\bar{\mathbf{G}}]^{-1}\{&\mathbf{C}(I - \bar{\mathbf{F}} - q\bar{T}\mathbf{I})\bar{\mathbf{Z}}(k)\\ &-\mathbf{C}\,\bar{\mathbf{G}}_p\mathbf{V}_p(k) - \varepsilon\bar{T}\,\mathrm{sgn}[\mathbf{C}\bar{\mathbf{Z}}(k)]\}.\end{aligned} \tag{19}$$

The vector $\mathbf{C}$ of the switching surface can be obtained using the pole assignment method or the optimal control method. When the optimal control method is used, the task is to design $\mathbf{C}$ by minimizing the objective function $\mathbf{J} = \sum_{k=0}^{\infty}[\bar{\mathbf{Z}}^{\mathrm{T}}(k)\tilde{\mathbf{Q}}\bar{\mathbf{Z}}(k)]$, where $\tilde{\mathbf{Q}}$ is a non-negative definite symmetric matrix. Similarly, the time-delay controller is designed directly from the time-delay differential equation and no approximation or hypothesis is involved, it tends to guarantee the stability of control systems, and is suitable for both small time delay and large time delay.

4. EXPERIMENT AND DATA PROCESSING

The feasibility and effectiveness of the proposed time-delay controller had been proven by simulation results.[9] In this paper, PZT patches are used as actuators, foil gauges were used as sensors, experiments are presented based on a digital signal processing (DSP) board. Firstly, an experimental setup using the DSP board is introduced. Subsequently, the measurement methods for signal and signal difference are presented.

4.1. Experiment System

In the experiment, two PZT patches are used as actuators, one PZT patch as a vibration exciter, and two foil gauges as sensors. The control mechanism of free and forced beam vibration are considered. For free vibration, the free end of beam has an initial displacement 0.04 m while the initial velocity is zero. For forced vibration, the PZT vibration exciter initiates beam vibration.

An experimental setup is constructed using DSP board (TMS320F2812). DSP deals with online computation of controllers in terms of the feedback signal from the foil gauge to obtain PZT voltage. Fig. 2 shows an experimental flow chart for forced vibration. For free vibration, the signal generator and PZT exciter in Fig. 2 are not in use. The details of signal flow and process are described as follows:

1. Excitation Loop: the signal generator generates an external excitation that is amplified by the PZT power amplifier and then goes into the PZT exciter. The flow chart of excitation loop is shown by the dashed line in Fig. 2.

2. Feedback Signal Loop: the signal collected from the foil gauge is amplified by a strain signal amplifier and then enters the analog digital converter (ADC) module in DSP.

3. Control Signal Loop: the voltage signal goes through the two channels of digital analog converter DAC module into the PZT power amplifier where it is amplified, and then channels into the two PZT actuators.

4. The DSP communicates with a computer via the serial communication interface (SCI) module which transfers the experimental data to the computer for storage and for post-processing.

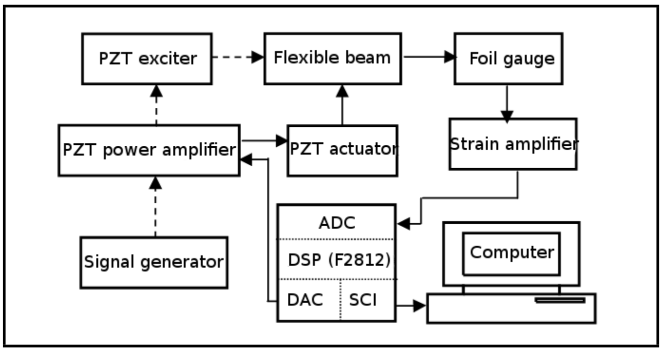

Figure 2. Flow chart of experiment system.

4.2. Signal Measurement

The controller described in Section 3 depends on the beam modal coordinate. Hence, a method to extract modal coordinate from the physical sensor measurements of foil gauges needs to be developed. In addition, the beam tip responses from foil gauge measurements with and without control will be compared to determine the efficiency. The methods required are introduced as follows.

The beam strain-curvature relationship can be expressed as

$$\varepsilon(x,t) = \frac{t_b}{2} y''(x,t); \tag{20}$$

where ϵ, t_b and y are the bending strain, thickness and beam transverse displacement, respectively. As mentioned, two foil gauges are used as sensors in the experiment. Since the first vibration mode has maximum strain at its fixed end while that of the second mode near the middle of beam, the two foil gauges are placed at these two positions at $x_1 = 37$ mm and $x_2 = 476$ mm , respectively. To extract the modal coordinate, the assumed mode method is applied where the beam response can be represented as $y(x,t) = \sum_{i=1}^{\infty} Y_i(x)\varphi_i(t)$ Because the beam response is dominated by its lower-order vibration modes, $y(x,t) \approx \sum_{i=1}^{2} Y_i(x)\varphi_i(t)$ is adopted in this paper. We can obtain the dominant modes by the modal cost analysis method to other geometries.[21] Using Eq. (20), the estimated modal displacement can be deduced as in Eq. (21)

After obtaining the modal displacement, the modal velocity can be determined using the tracking-differentiator given in Section 4.3. From modal coordinate thus obtained, the controlling system can be calculated.

Subsequently, the strain measurements from the two foil gauges can be transformed into the transverse displacement of the beam by Eq. (22) Taking $x = L$ in Eq. (22), where L is the length, the beam tip response can be approximately from Eq. (21).

4.3. Signal Difference

The states for an active controller system, i.e. displacement and velocity, are required in the feedback control. Because the velocity signal (also called the differential signal) cannot be measured directly from sensors in practice, it should be estimated from the physical measurements, and then be used to calculate the control forces. In an early attempt, it was found that the foil gauge signal may contain high-frequency noise due to mechanism and electricity disturbances; hence, the differential signal derived from the classical interpolation method is disorganized. As a result, the tracking differentiator is adopted and it is able quickly tracking the input signal and giving out high-quality differential signal. The tracking differentiator in discrete form is[22]

$$\begin{cases} \bar{x}_1(k+1) = \bar{x}_1(k) + \bar{T}\bar{x}_2(k) \\ \bar{x}_2(k+1) = \bar{x}_2(k) + \bar{T}fst(\bar{x}_1(k), \bar{x}_2(k), u(k), \bar{r}, \bar{h}) \end{cases}; \tag{23}$$

where $u(k)$ is the input signal at the moment k, $\bar{x}_1$ is the tracking signal of $u(k)$, $\bar{x}_2$ is the estimated differential signal of $\bar{x}_1$, $\bar{T}$ is the sampling period, $\bar{r}$ is a parameter determining the tracking speed, and $\bar{h}$ is a parameter determining the filter effect when the input signal is polluted by noise. The variable fst is given in Reference.[22]

5. NUMERICAL SIMULATIONS AND EXPERIMENTAL STUDIES

A beam made of aluminum alloy is used in the experiment shown in Fig. 3. The length, width and thickness are 900 mm, 35 mm, and 1.50 mm, respectively. Material properties of the beam are as follows: Young's elastic modulus $E_p = 69$ GPa, Poisson's ratio $v_p = 0.3$ and density $\rho_p = 2.7 \times 10^3$ kg/m^3. The first two natural frequencies of the beam determined from the experiment are 1.4947 Hz and 9.3679 Hz, respectively, and the corresponding modal damping ratios are 0.012 and 0.0055.

In the experiment, one PZT patch is used as an exciter to initiate beam vibration and the other two PZT patches are used as actuators to control vibration. The PZT patches have identical sizes, 60 mm $\times$ 15 mm $\times$ 0.5 mm. The PZT exciter is placed near the root of beam at $\tilde{x}_{pa} = 77$ mm and $\tilde{x}_{pb} = 137$ mm. One PZT actuator (denoted as Actuator I) was attached to the other side of the beam at $\tilde{x}_{1a} = 82$ mm and $\tilde{x}_{1b} = 142$ mm. The time delay of Actuator I is denoted by λ_1 . Another PZT actuator (denoted as Actuator II) was attached near the beam midpoint at $\tilde{x}_{2a} = 375$ mm and $\tilde{x}_{2b} = 435$ mm, and the time delay is denoted by λ_2 (see Fig. 1). The PZT material parameters are: Young's modulus 63 GPa, Poisson's ratio 0.35 and piezoelectric strain constants 1.75×10^{-10} m/V. For the differentiator, $\bar{r} = 1000$ and $\bar{h} = 0.008$ are taken.

The inherent delays in the system may have small effect on control efficiency and can be ignored in control design. From Fig. 4, we can see that the beam vibration can be effectively suppressed when the inherent delays in the system are not considered. So, the experiment system used in this paper may be regarded as a non-time-delay control system. We think that just under this condition, the effect of time delay on control systems and the effectiveness of delayed feedback control method may possibly be studied. The time delay used in the experimental studies of this paper is voluntarily introduced in the

$$\begin{bmatrix} \varphi_1(t) \\ \varphi_2(t) \end{bmatrix} = \frac{2}{t_b} \begin{bmatrix} Y''_1(x_1) & Y''_2(x_1) \\ Y''_1(x_2) & Y''_2(x_2) \end{bmatrix}^{-1} \begin{bmatrix} \varepsilon(x_1,t) \\ \varepsilon(x_2,t) \end{bmatrix}; \tag{21}$$

$$y(x,t) = \frac{2}{t_b} \begin{bmatrix} Y_1(x) & Y_2(x) \end{bmatrix} \begin{bmatrix} Y''_1(x_1) & Y''_2(x_1) \\ Y''_1(x_2) & Y''_2(x_2) \end{bmatrix}^{-1} \begin{bmatrix} \varepsilon(x_1,t) \\ \varepsilon(x_2,t) \end{bmatrix}; \tag{22}$$

Figure 3. Photo of experiment beam.

control system by means of adding arbitrary delayed times to control input.

5.1. Results of Forced Vibration Case

The forced vibration control is investigated in this section. In the experiment, the signal generator generates a sine voltage signal with frequency 1.524 Hz and amplitude 5 V. The sine signal is amplified fifteen times by the PZT power amplifier and it then goes into the PZT exciter in order to introduce beam forced vibration. The two PZT actuators are used for controlling the vibration. The optimal control strategy is applied as control. From Eq. (10), large $\bar{\mathbf{Q}}_1$ means that the corresponding state will be quickly suppressed and large $\bar{\mathbf{Q}}_2$ will penalize the control inputs. So increasing $\bar{\mathbf{Q}}_1$ or decreasing $\bar{\mathbf{Q}}_2$ within the capacity of the actuator, the better control effect will be obtained. In the controller design, the weighting matrices in Eq. (10) are chosen as $\bar{\mathbf{Q}}_1 = diag[100, 100, 1, 1]$ and $\bar{\mathbf{Q}}_2 = diag[4 \times 10^{-6}, 4 \times 10^{-6}]$ because the electrical field intensity keeps linear relationship with the strain of PZT only when external electrical field intensity does not exceed 150 V.

The no-delay controller design is applied to control the system without time delay. The beam tip responses and the PZT applied voltage are shown in Fig. 4. The dotted line refers to the results with no control while the solid line refers to the results with control. Fig. 4a are the simulation results, and Fig. 4b are the experimental ones. As observed in Fig. 4b1, the maximum amplitude without control is 0.0262 m and that with control is 0.0108 m. The beam vibration could be effectively suppressed.

The time-delay controller is subsequently investigated here. Two cases are considered: one with a short time delay ($\lambda_1 = 0.05\text{s}, \lambda_2 = 0.04\text{s}$), and another with a long time delay ($\lambda_1 = 0.2\text{s}, \lambda_2 = 0.1\text{s}$). A time-delay controller can be designed with reference to the method described in Section 3.2. The results using a time-delay controller for controlling beam vibration are shown in Figs. 5 and 6, where the dotted line donates the results without control, and the solid line donates the results with control. Figs. 5b1 and 6b1 show that the amplitudes with control are 0.0112 m, 0.013 m, respectively. We can observe that the beam vibration can be suppressed effectively by the time-delay controller, and the proposed time-delay controller is also applicable to short and long time delays.

5.2. Results of Free Vibration Case

Further examples for the control of beam free vibration are presented here to demonstrate the effectiveness of the proposed time-delay controller. An external force is applied to create an initial displacement 0.04 m with zero initial velocity at the free end of the beam. With such conditions, Actuators I and II are used to control the free vibration. A control strategy based on the variable structure control method is used. In the controller design, $\epsilon = 0.01$ and $q = 10$ are chosen in Eq. (19). $\tilde{\mathbf{Q}}$ is chosen as $\tilde{\mathbf{Q}}(1,1) = 100$, $\tilde{\mathbf{Q}}(2,2) = 100$, $\tilde{\mathbf{Q}}(4+l_1, 4+l_1) = 5 \times 10^{-7}$, $\tilde{\mathbf{Q}}(4+l_1+l_2, 4+l_1+l_2) = 5 \times 10^{-7}$ with other elements being zero.

A short time delay ($\lambda_1 = 0.05\text{s}, \lambda_2 = 0.08\text{s}$) and a long time delay ($\lambda_1 = 0.2\text{s}, \lambda_2 = 0.3\text{s}$) are considered. A time-delay controller is designed using the method described in Section 3.3. Numerical and experimental results are shown in Figs. 7 and 8 where the dotted line donates the results without control, and the solid line donates the result with control. From Figs. 7b1 and 8b1, the logarithmic decay ratios of the first period are 0.0179 and 0.0145, respectively. As observed in Figs. 7 and 8, the time-delay controller is able to control the beam vibration effectively and the experiment results agree better with respect to simulation.

6. CONCLUSION

In this paper, delayed feedback control for vibration of a flexible beam is studied numerically and experimentally. Time-delay controllers are proposed to suppress the beam vibration. The discrete optimal control method and the discrete variable structure control method are used for designing the controllers. An experiment system based on a DSP board is introduced. The numerical and experimental results show that the proposed time-delay processing method is effective in suppressing beam vibration. It is applicable to any time delays.

ACKNOWLEDGEMENTS

This work was supported by the Natural Science Foundation of China (11002087, 11272202), the Specialized Research Fund for the Doctoral Program of Higher Education of China (20110073110008), and the Key Scientific Project of Shanghai Municipal Education Commission (14ZZ021). should be revised to This work was supported by the Natural Science Foundation of China (11132001, 11272202 and 11472171), the Specialized Research Fund for the Doctoral Program of Higher Education of China (20110073110008), the Key Scientific Project of Shanghai Municipal Education Commission (14ZZ021), and the Natural Science Foundation of Shanghai (14ZR1421000).

REFERENCES

[1] Hu, H. Y. and Wang, Z. H. Dynamics of Controlled Mechanical Systems with Delayed Feedback, Springer-Verlag, Berlin, (2002).

[2] Abdel-Rohman, M. Time-delay effects on active damped structures, *J. Eng. Mech.*, **113**(11), 1709–1719, (1987).

[3] Chung, L. L., Reinhorn, A. M., and Soong, T. T. Experiments on active control of seismic structures, *J. Eng. Mech.*, **114**(2), 241–256, (1988).

[4] McGreery, S., Soong, T. T., and Reinhorn, A. M. An experiments study of time delay compensation in active structural control, *Proc. Sixth International Modal Analysis Conference, SEM*, 1733–1739, (1988).

[5] Cai, G. P. and Huang, J. Z. Optimal control method for seismically excited building structures with time-delay in control, J. Eng. Mech., 128 (6), 602612, (2002).

[6] Cai, G. P., Huang, J. Z., and Yang, S. X. An optimal control method for linear systems with time delay, *Comput. Struct.*, **81**(15), 1539–1546, (2003).

[7] Chen, L. X. and Cai, G. P. Optimal control of a flexible beam with multiple time delays, *J. Vib. Control.*, **15**(10), 1493–1512, (2009).

[8] Sun, J. Q. A method of continuous time approximation of delayed dynamical systems, *Commun. Nonlinear. Sci.*, **14**(4), 998–1007, (2009).

[9] Xu, J. and Chung, K. W. Effects of time delayed position feedback on a van der Pol-Duffing oscillator, *Phys. D*, **180**(1), 17–39, (2003).

[10] Daqaq, M., Alhazza, K., and Arafat, H. Non-linear vibrations of cantilever beams with feedback delays, *Int. J. Nonlin. Mech.*, **43**(9), 962–978, (2008)

[11] Hosek, M. and Olgac, N. A single-step automatic tuning algorithm for the delayed resonator vibration absorber, *IEEE/ASME Trans. Mechatron*, **7**(2), 245–255, (2002).

[12] Cavdaroglu, M. E. and Olgac, N. Full-state feedback controller design with delay scheduling for cart-and-pendulum dynamics, *Mechatronics*, **21**(1), 38–47, (2011).

[13] Liu, B., Haraguchi, M., and Hu, H. Y. A new reduction-based LQ control for dynamic systems with a slowly time-varying delay, *Acta Mech. Sin.*, **25**(4), 529–537, (2009).

[14] Cai, G. P. and Lim, C. W. Optimal tracking control of flexible hub-beam system with time delay, *Multibody Syst. Dyn.*, **16**(4), 331–350, (2006).

[15] Yuan, F. Effects of delayed feedback control on stability in the cantilever pipe conveying fluid, *Master Thesis*, Tongji University, China, (2008). (in Chinese)

[16] Wang, Z. H. and Hu, H. Y. Stabilization of vibration systems via delayed state difference feedback, *J. Sound Vib.*, **296**(1–2), 117–129, (2006).

[17] Xu, J., Chung, K. W., and Chan, C. L. An efficient method for studying weak resonant double Hopf bifurcation in nonlinear systems with delayed feedbacks, *SIAM J. Appl. Dyn. Syst.*, **6**(1), 29–60, (2007).

[18] Crawley, E. F. and Anderson, E. H. Detailed models of piezoceramic actuation of beams, *J. Intel. Mat. Syst. Str.*, **1**(1), 4–25, (1990).

[19] Sun, Z. Q. *Theory and Application of Computer Control*, Tsinghua University Press, Beijing, (1989). (in Chinese)

[20] Gao, W. B. *Theory and Design Method of the Variable Structure Control*, Science Press, Beijing, (1996). (in Chinese)

[21] Zhang, M. and Cai, G. P. Modal cost reduction and active control of a flexible plate. *J. Dyn. Control*, **6**(4), 348–352, (2008). (in Chinese)

[22] Han, J. Q. and Yuan, L. L. The discrete form of tracking-differentiator, *J. Syst. Sci. Math. Sci.*, **19**(3), 268–273, (1999). (in Chinese)

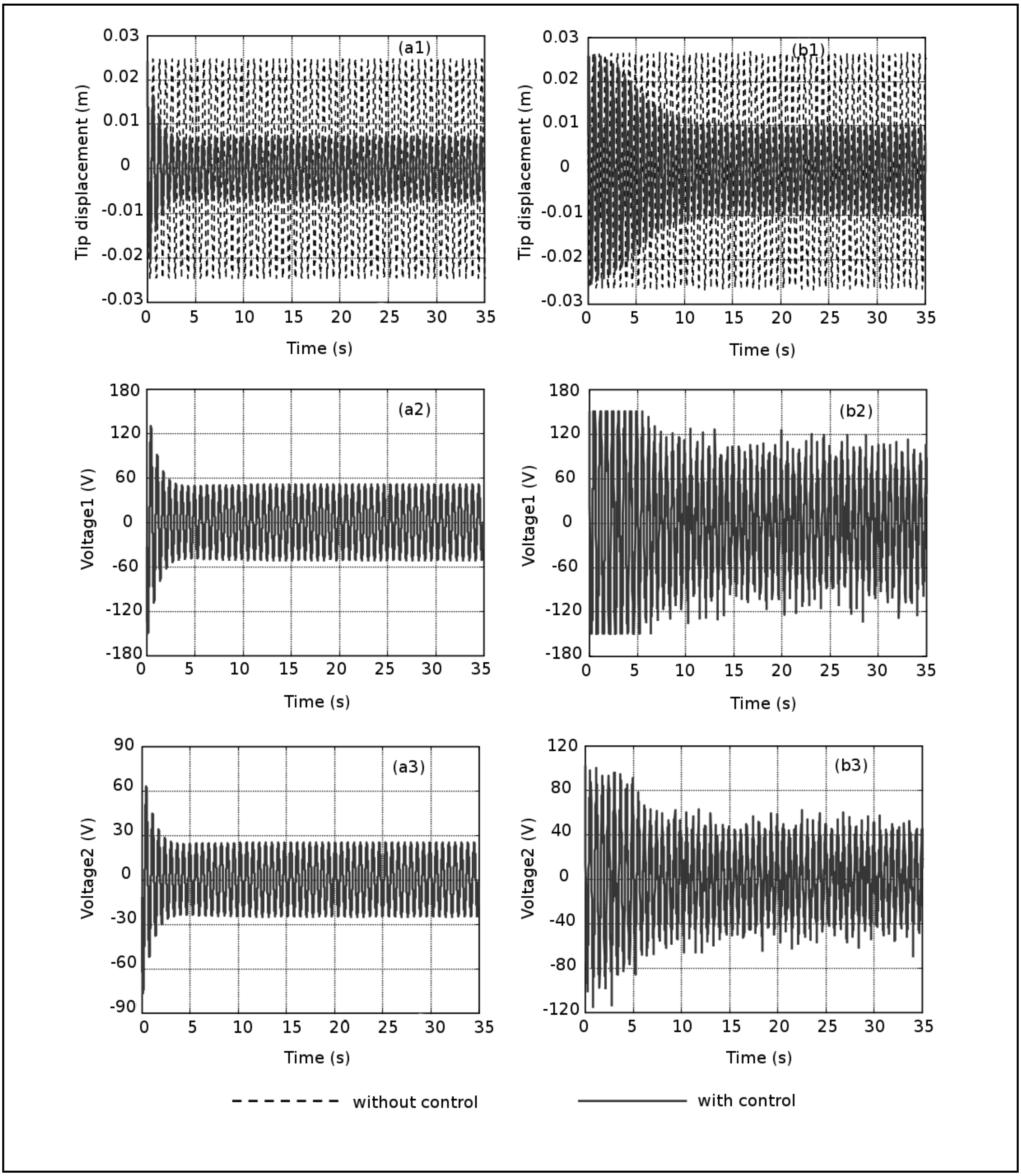

Figure 4. Tip response of the beam and applied voltages on the two actuators (without time delay; optimal controller): (a) simulation result, (b) experimental result.

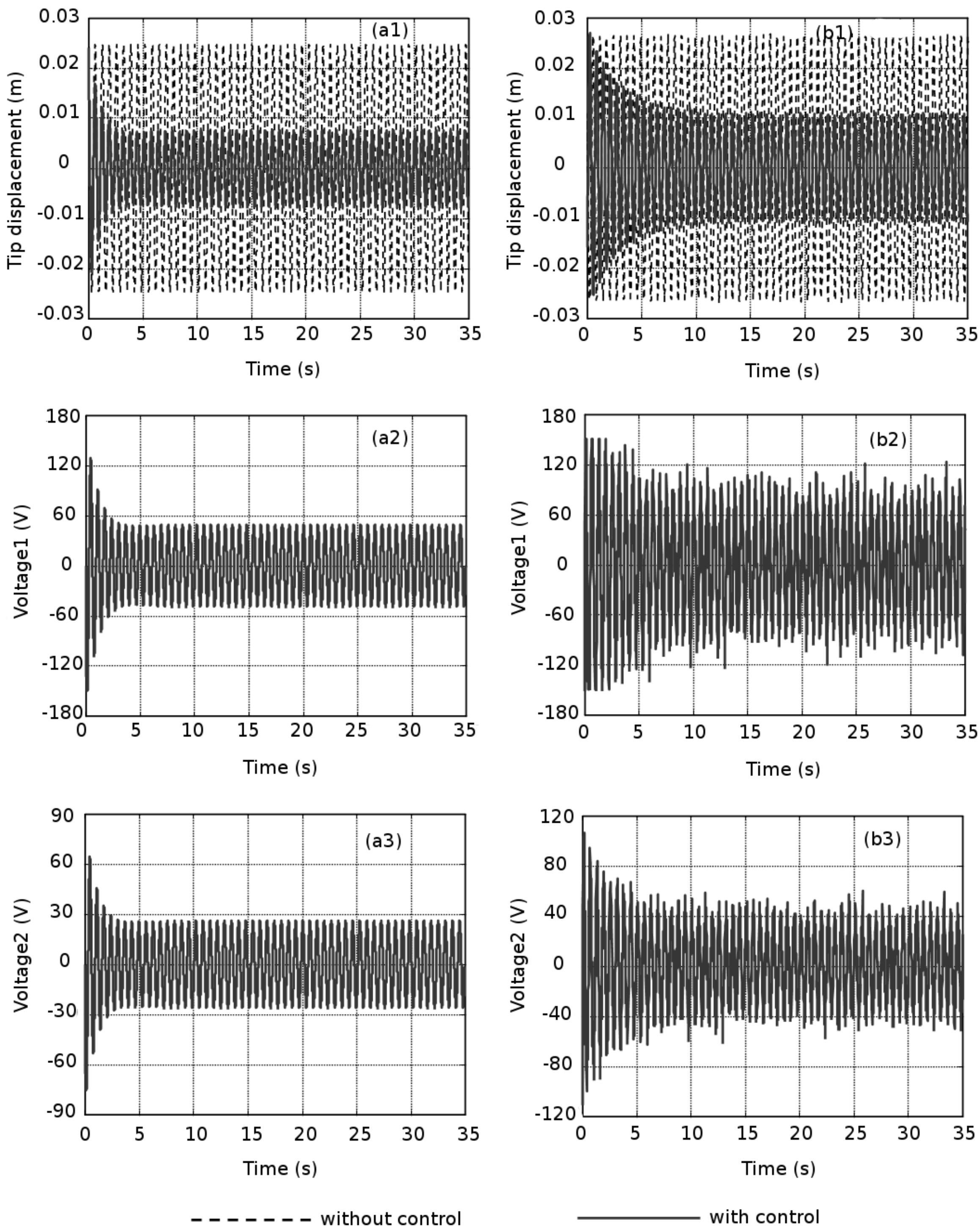

Figure 5. Tip response of the beam and applied voltages on the two actuators ($\lambda_1 = 0.05$ s, $\lambda_2 = 0.04$ s; time-delay optimal controller): (a) simulation result, (b) experimental result.

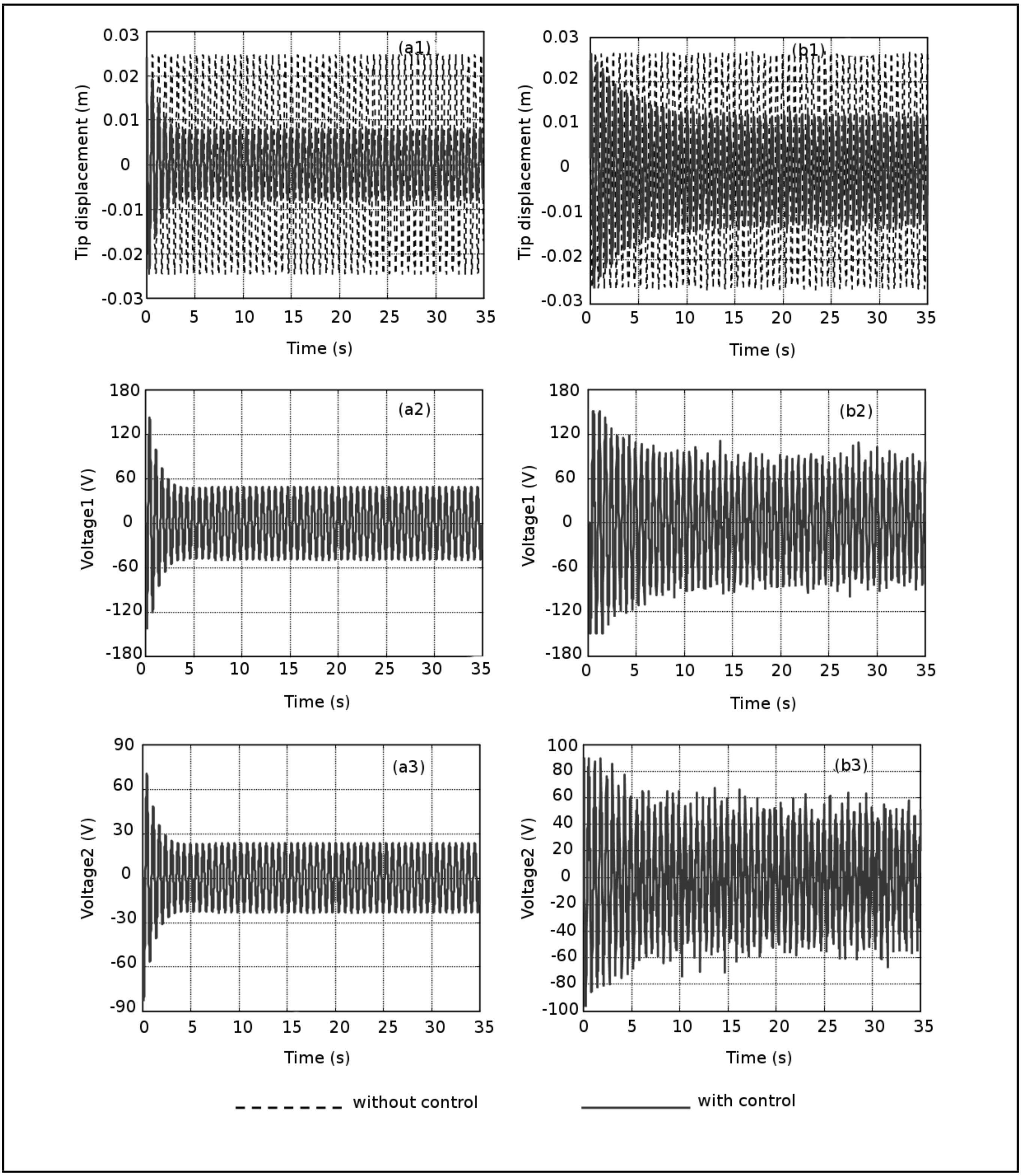

Figure 6. Tip response of the beam and applied voltages on the two actuators ($\lambda_1 = 0.2$ s, $\lambda_2 = 0.1$ s; time-delay optimal controller): (a) simulation result, (b) experimental result.

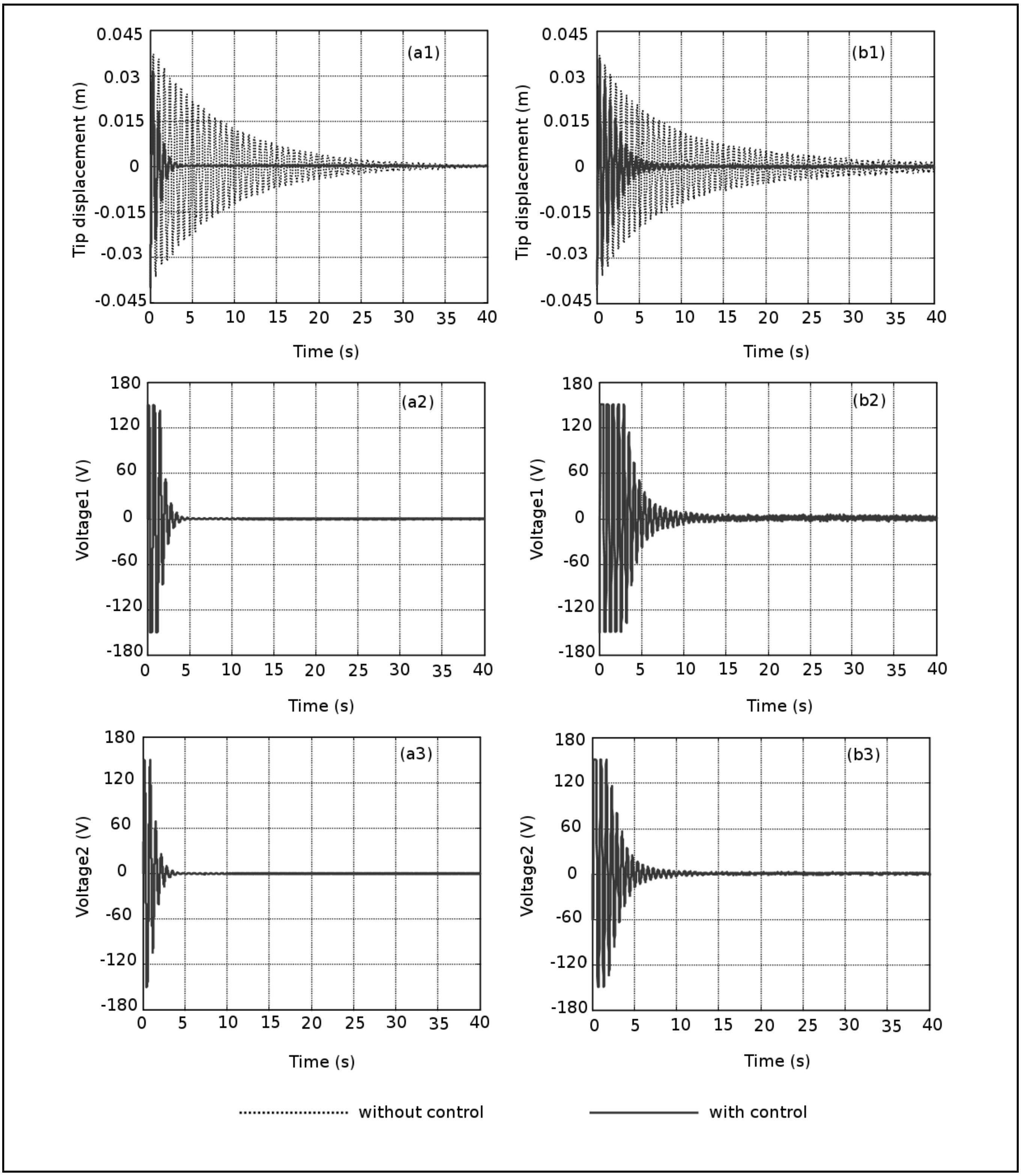

Figure 7. Tip response of the beam and applied voltages on the two actuators ($\lambda_1 = 0.05$ s, $\lambda_2 = 0.08$ s; time-delay variable structure controller): (a) simulation result, (b) experimental result.

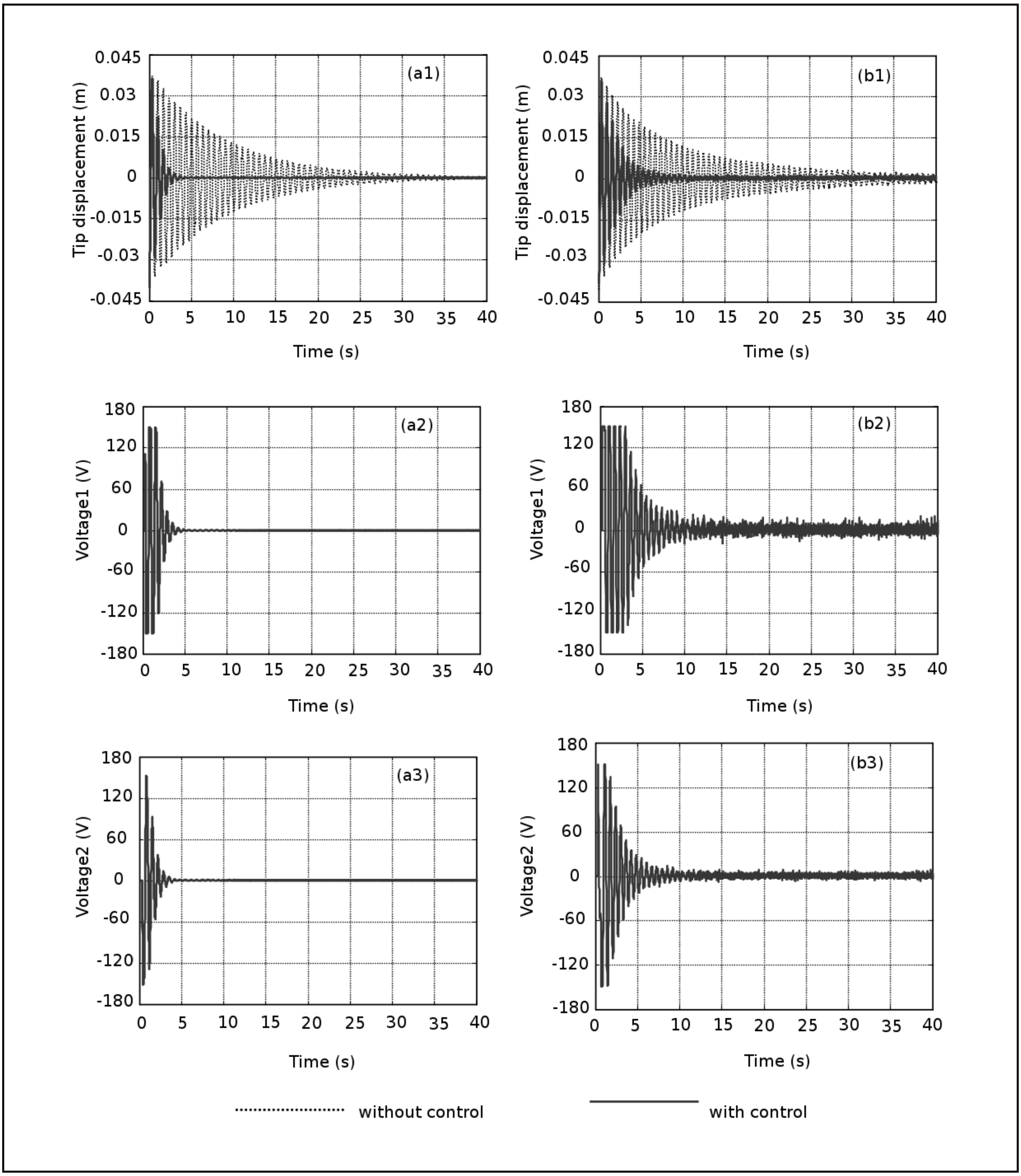

Figure 8. Tip response of the beam and applied voltages on the two actuators ($\lambda_1 = 0.2$ s, $\lambda_2 = 0.3$ s; time-delay variable structure controller): (a) simulation result, (b) experimental result.